Terra Nova

doi: 10.1111/ter.12182

Magmatism at continental passive margins inferred from Ambient-Noise Phase-velocity in the Gulf of Aden

Félicie Korostelev,[1] Sylvie Leroy,[1] Derek Keir,[2] Cornelis Weemstra,[3] Lapo Boschi,[1] Irene Molinari,[4] Abdulhakim Ahmed,[1,5] Graham W. Stuart,[6] Frédérique Rolandone,[1] Khaled Khanbari[7] and Ali Al-Lazki[8]

[1]*Sorbonne Universités, UPMC Univ Paris 06, CNRS, Institut des Sciences de la Terre de Paris (ISTEP), 4 place Jussieu, Paris 75005, France;* [2]*National Oceanography Centre Southampton, University of Southampton, Southampton SO14 3ZH, UK;* [3]*Department of Geoscience and Engineering, Delft University of Technology, Stevinweg 1, Delft 2628 CN, The Netherlands;* [4]*Department of Earth Sciences, ETH Zurich, Zurich, Switzerland;* [5]*Seismological and Volcanological Observatory Center, Dhamar, Yemen;* [6]*School of Earth and Environment, University of Leeds, Leeds, UK;* [7]*Yemen Remote Sensing and GIS Center, Sana'a University, Sana'a, Yemen;* [8]*Sultan Qaboos University, Muscat, Oman*

ABSTRACT

Non-volcanic continental passive margins have traditionally been considered to be tectonically and magmatically inactive once continental breakup has occurred and seafloor spreading has commenced. We use ambient-noise tomography to constrain Rayleigh-wave phase-velocity maps beneath the eastern Gulf of Aden (eastern Yemen and southern Oman). In the crust, we image low velocities beneath the Jiza-Qamar (Yemen) and Ashawq-Salalah (Oman) basins, likely caused by the presence of partial melt associated with magmatic plumbing systems beneath the rifted margin. Our results provide strong evidence that magma intrusion persists after breakup, modifying the composition and thermal structure of the continental margin. The coincidence between zones of crustal intrusion and steep gradients in lithospheric thinning, as well as with transform faults, suggests that magmatism post-breakup may be driven by small-scale convection and enhanced by edge-driven flow at the juxtaposition of lithosphere of varying thickness and thermal age.

Terra Nova, 28: 19–26, 2016

Introduction

Mechanical faulting and ductile stretching, as well as magma intrusion, accommodate extension of the lithosphere beneath rifts and can lead to continental breakup (McKenzie, 1978). During the early stages of rifting, crustal extension is commonly thought to occur mainly on border faults (e.g. Bellahsen *et al*., 2006). As the rift widens, extension commonly localizes in-rift to small offset fault networks, and in magma-rich settings to magma intrusion in axial volcanic segments (Ebinger and Casey, 2001). Once breakup occurs and a new mid-ocean ridge forms, the conjugate rifted passive margins at the edges of the continents are commonly assumed to be tectonically and magmatically inactive. However, it is becoming increasingly recognized that the continental margins may remain active after breakup (Ebinger and Belachew, 2010; Pallister *et al*., 2010; Rooney *et al*., 2014) and continue to accommodate extension and modify the thermal structure and composition of the crust and upper mantle (Bellahsen *et al*., 2013a; Watremez *et al*., 2013). Despite its importance, we have few constraints on the distribution and time-scales over which magmatism persists at rifted margins. In order to constrain the magma plumbing system beneath a rifted margin, we use ambient-seismic-noise tomography to image the Rayleigh-wave phase-velocity structure of the crust and upper mantle beneath the young rifted margin on the northern side of the Gulf of Aden in Yemen and southern Oman (Fig. 1).

Fault-related sediment deposits in Oman and Yemen suggest rifting began at about 34 Ma along the whole Gulf (e.g. Leroy *et al*., 2012; Robinet *et al*., 2013; Fig. 1), approximately coeval with ~25–31 Ma opening in the Afar region (e.g. Wolfenden *et al*., 2005; Ayalew *et al*., 2006; Stab *et al*., 2015). Rifting was associated with the development of 2-km deep grabens in the proximal part of the margin, with a present relief of 3000–4000 m between the submarine distal domain (at 2000 m deep) and the subaerial uplifted Yemen and Oman shoulders (Leroy *et al*., 2010a; Watremez *et al*., 2011; Figs 1 and 2). A prior stage of extension in the Cretaceous created the Jiza-Qamar and Gardafui grabens located in Yemen and in the south of Socotra Island (Fig. 1b); these were reactivated during the most recent extension between 34 and 18 Ma (Leroy *et al*., 2012). Extension occurs above a warm mantle of potential temperature (Tp) 1450 °C in the west (Rooney *et al*., 2012; Ferguson *et al*., 2013) and likely above normal mantle of Tp 1350 °C in the east (Lucazeau *et al*., 2010; Bellahsen *et al*., 2013a; Rolandone *et al*., 2013). Rifting above warm mantle in the west is associated with the production of voluminous flood basalts on the Yemeni plateaus synchronous with the onset of extension and the formation of volcanic margins with characteristic seaward-dipping reflectors (SDR) during breakup (Tard *et al*., 1991; Leroy *et al*., 2012; Ahmed *et al*., 2013; Korostelev *et al*., 2014; Fig. 1b). In Central Yemen, rifting

Correspondence: Félicie Korostelev, CNRS ISTEP-UPMC, Univ. Paris 06, Paris, France. Tel.: +00 33 0144275260; e-mail: felicie.korostelev@gmail.com

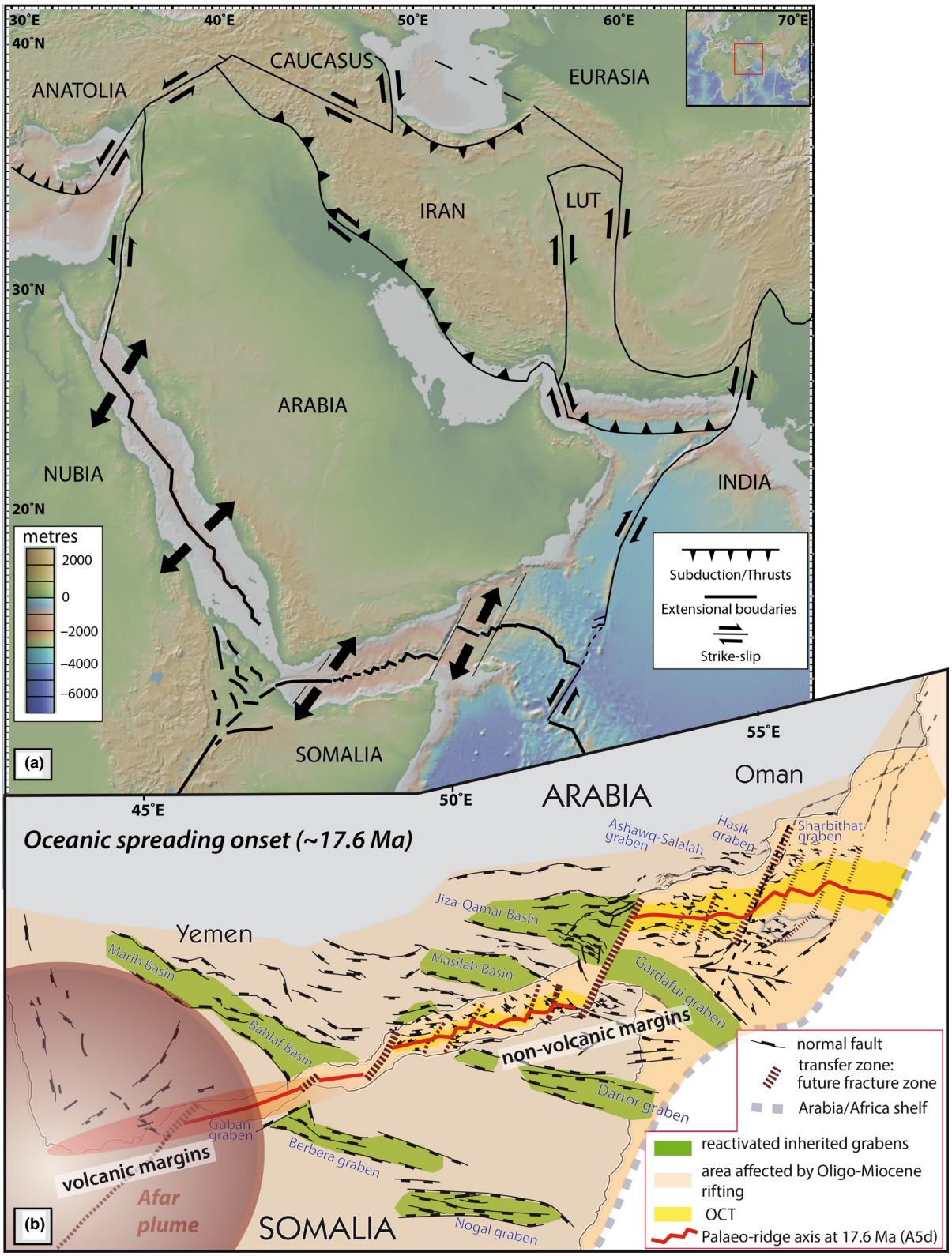

Fig. 1 (a) Topography and bathymetry of the Arabian plate region from http://www.geomapapp.org and Ryan *et al.* (2009). Black arrows show relative plate motions. (b) Reconstructed map just before the onset of oceanic spreading in the Gulf of Aden (17.6 Ma) (from Leroy *et al.* (2012)), showing the locations of the pre-existing basins that were reactivated during the last episode of rifting leading to continental breakup and oceanic spreading.

occurs above warm mantle without SDR formation but with lacustrine syn-rift sedimentation (a few meters). Rifting in the eastern part of the Gulf is associated with turbiditic syn-rift sedimentation (hundreds of meters) (Leroy *et al.*, 2012; Robinet *et al.*, 2013).

From ~19 Ma to present, evidence for magmatism in the form of volcanism is recorded along most of the Gulf of Aden (Leroy *et al.*, 2010b), with Quaternary-Recent volcanic centers common in western Yemen (Manetti *et al.*, 1991; Korostelev *et al.*, 2014), localized to near the Masilah graben in central Yemen (Korostelev *et al.*, 2015a) and observed at the foot of the margin offshore Oman in the eastern part of the Gulf of Aden (Lucazeau *et al.*, 2009; Autin *et al.*, 2010; Figs 1 and 2).

Both the continental rifted margin and the ocean ridge are segmented by major fracture zones. The Alula-Fartak fracture zone (AFFZ) has a maximum lateral offset of 180 km and divides the Jiza-Qamar Gardafui pre-existing basin (d'Acremont *et al.*, 2005, 2010; Leroy *et al.*, 2012; Bellahsen *et al.*, 2013b); the active spreading ridge is localized at its northern edge in the east and at its southern edge in the west (Fig. 1b). The crustal thickness beneath the southern Arabia continental margin varies from 35–45 km beneath most of its relatively undeformed northern

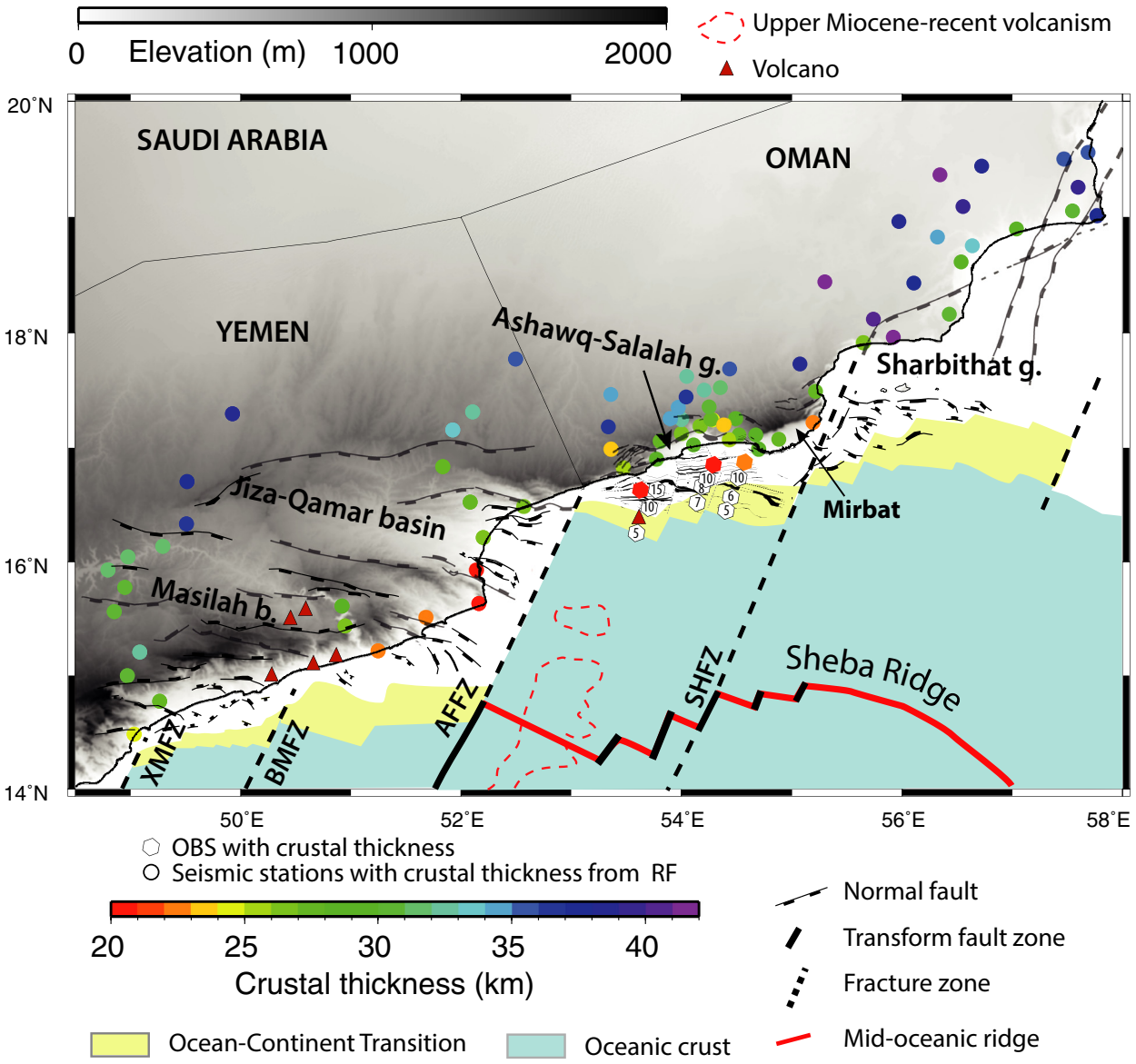

Fig. 2 Structure of the northern margin of the eastern Gulf of Aden. Crustal thickness is indicated by coloured dots at the locations of seismic stations and estimated from receiver functions (Tiberi *et al.* (2007) and Leroy *et al.* (2012) in Dhofar, Korostelev *et al.* (2015b) in Yemen and eastern Oman) and by diamonds from Ocean Bottom Seismometers (OBS; Leroy *et al.*, 2010a; Watremez *et al.*, 2011). XMFZ, Xiis-Mukalla fracture zone; BMFZ, Bosaso-Masilah fracture zone; AFFZ, Alula-Fartak fracture zone; SHFZ, Socotra-Hadbeen fracture zone; Masilah b., Masilah basin; Sharbithat g., Sharbithat graben.

edge to 25–30 km beneath the rifted margin at the coast (Tiberi *et al.*, 2007; Leroy *et al.*, 2012; Korostelev *et al.*, 2015a; Fig. 2). Crustal thinning occurs seaward, with ~20-km-thick crust observed beneath the southern edge of the Jiza-Qamar basin and 5-km-thick crust beneath the ocean–continent transition (OCT) (d'Acremont *et al.*, 2006; Leroy *et al.*, 2010b; Watremez *et al.*, 2011; Fig. 2).

Data

Our dataset is based on continuous recordings from 142 seismic stations, mainly from temporary networks of broadband seismometers (Fig. 2). The data quality selection followed two steps: (i) selection of pairs of stations that recorded simultaneously for at least 6 months, and (ii) comparison of the measured pairs, keeping those that showed a good fit (Korostelev *et al.*, 2015b). The duration of the cross-correlated signal thus varies by 6–18 months depending on the station pair. The method is described in the supplementary material (Figures S1 and S2 in Data S1).

Results

We computed phase-velocity maps for periods between 7 and 30 s, and present four examples at 10, 12.5, 17 and 20.5 s (Fig. 3). The images show Rayleigh-wave phase-velocity perturbations relative to the mean Rayleigh-wave phase-velocity. According to, for example, Lebedev and Van Der Hilst (2008) and Fry *et al.* (2010), 10 s Rayleigh waves are most sensitive to depths less than 20 km (upper and mid- crust), while 12.5–15.5 s periods are most sensitive to depths of 10–40 km (primarily the lower crust). The 17–20.5 s periods are most sensitive to depths of 20–25 km and have some sensitivity to depths of 50–60 km (uppermost mantle). Given that the lithosphere in the region is estimated to be 150 km thick (Rolandone *et al.*, 2013), we are primarily imaging the uppermost mantle lithosphere in our longer-period maps. In the supplementary material, we provide some examples of surface-wave depth-sensitivity functions (Figure S3 in Data S1).

The locus of major velocity anomalies is fairly constant from 10 to 12.5 s to the east of the Alula-Fartak fracture zone (AFFZ; Fig. 3). We image fast velocity perturbations beneath the eastern part of the Ashawq-Salalah graben beneath the Mirbat plain near the Socotra-Hadbeen fracture zone and in the Sharbithat area (Figs 1, 2 and 3). Fast velocity perturbations are also present beneath the Jiza-Qamar basin at 17 and 20.5 s in between the major faults.

At the 12.5 s period, the slow anomalies are concentrated in the center of the Jiza-Qamar basin and in the north of the Ashawq-Salalah graben (Fig. 3). At the 20 s period we also image slow anomalies in central Yemen at 49°E (Fig. 3).

The magnitudes of several of the distinct velocity perturbations vary with period. For example, beneath the Mirbat area (Oman, Fig. 2), the fast anomaly increases in magnitude from ~3% at 12.5 s to 9% at 17–20.5 s (Fig. 3). The slow anomaly beneath the Jiza-Qamar basin is mostly more than −10% at 10 s, whereas at 12.5 s a larger proportion of the anomaly is –6% (Fig. 3).

The slow anomalies beneath the western part of the Ashawq-Salalah graben and beneath central Yemen correlate well with the areas of surface volcanism known offshore and onshore respectively (Figs 2 and 3). In addition, the shallower low-velocity anomaly located in the center of the eastern part of the graben corresponds well to the locus of maximum thickness of sediment infill of the Cretaceous basin in between the major faults (Figs 2 and 3). Sediment thickness is greatest in the east, where plate thinning is likely greatest (Brannan *et al.*, 1997; Hakimi and Abdullah, 2014).

The values of the deep slow anomalies imaged using ambient noise are also in general agreement with the values of low crustal shear velocities (3.15–3.45 km s^{-1} from Pasyanos and Nyblade, 2007) in the crust, and their spatial extent correlates well with low velocities in the mantle constrained using P-wave teleseismic tomography (Korostelev *et al.*, 2015a). The ambient noise provides an additional constraint on the depth of the anomaly in the upper mantle (20.5 s, Fig. 3).

Discussion

Seismic-wave velocity is known to be affected by the temperature and chemical composition of the medium of propagation (crustal and mantle rocks) as well as by the concentration of fluids, such as partial melt and geothermal fluids (e.g. Christensen and Mooney, 1995; Karato *et al.*, 2003). We image slow velocities beneath zones of known active volcanism in southern Yemen (Fig. 1 and 2, see the locations of volcanoes), in agreement with the hypothesis that the major surface-wave slow anomalies are associated with magmatism. The magnitudes of the anomalies and their spatial distribution in regions where extension has occurred suggest that magmatic processes currently modify the crust beneath the flanks of continental rifted margins. Beneath the proximal margin, geological studies suggest early border faults were active at 34 Ma but not associated with much volcanism; yet our velocity maps suggest that magmatic systems are currently active in these regions ~20 Ma post-breakup.

The slow anomalies in our phase-velocity maps beneath the Jiza-Qamar graben are observed in the lower crust, with higher amplitude in the north (Fig. 3; period = 10 and 12.5 s). These velocities could be indicative of fluids (especially partial melt) in the crust beneath the proximal grabens of the Gulf of Aden northern margin (Jiza-Qamar, Ashawq-Salalah and Sharbithat grabens) where surface volcanism is lacking (Fig. 2). Basuyau *et al.* (2010) identified localized slow velocities at around 60 km depth, interpreted as zones of partial melt, which supports the inference that our overlying crustal slow anomalies may be caused by regions of intrusion lacking eruption. The highly segmented continental margin of the Gulf of Aden, and especially the 180 km long offset of the AFFZ, could localize the transport of fluids through the lithosphere. Magmatism and particularly dike intrusion is common in transform fault zones (e.g. Gudmundsson, 1987, 1995). In addition, it has been demonstrated that uplift lessens the potential energy and may favour the

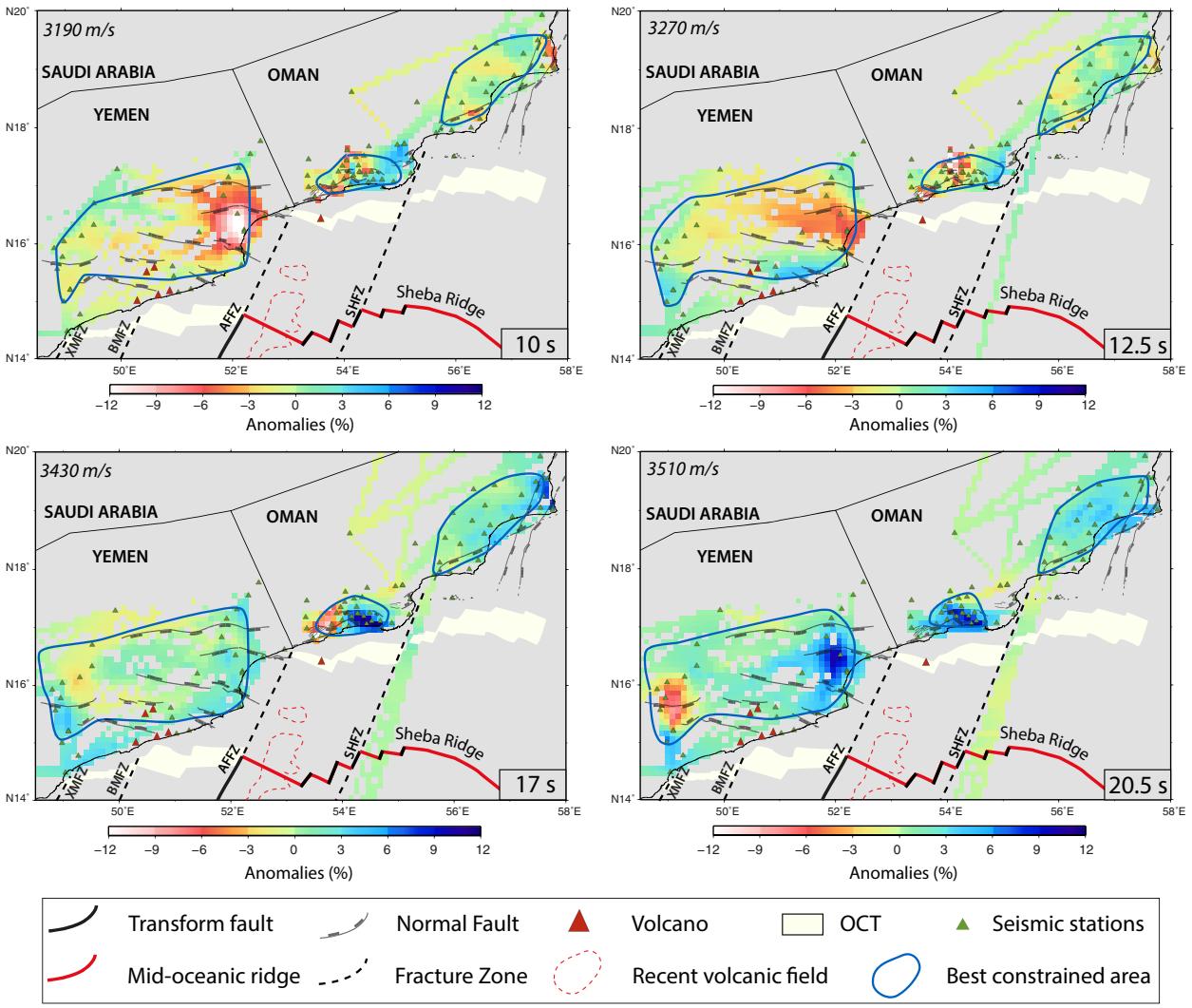

Fig. 3 Maps of phase velocity anomalies (% perturbation with respect to average) resulting from inversion of ambient noise dispersion data. The average velocity for each period is indicated on the top left of each image. Main tectonic structures and the ocean-continent transition (OCT) are drawn. XMFZ, Xiis-Mukalla fracture zone; BMFZ, Bosaso-Masilah fracture zone; AFFZ, Alula-Fartak fracture zone; SHFZ, Socotra-Hadbeen fracture zone. The solid blue lines delimit the best-constrained areas. According to e.g. Lebedev and Van Der Hilst (2008) and Fry *et al.* (2010), 10-s Rayleigh waves are most sensitive to depths less than 20 km (upper and mid crust) while 12.5–15.5 s periods are most sensitive to depths of 10–40 km (primarily the lower crust). The 17–20.5 s periods are most sensitive to depths of 20–25 km and have some sensitivity to depths of 50–60 km (uppermost mantle).

accumulation of fluids, if available (Gudmundsson, 2000). Dike migration could be arrested and deflected into sills by sharp horizontal layering such as the base of the crust, the basement–sediment interface, and sedimentary layering within the basin (Gudmundsson, 2011). The 4-km-thick sediments of the Jiza-Qamar basin located along a major transform fault zone and uplifted after the breakup are thus likely to be a favourable location for diking and magmatism.

Figure 4 shows an interpreted cross-section through the Jiza-Qamar basin based on our phase-velocity models. The present-day crustal thickness and basin fill, with 4-km-thick Cretaceous sediments, are inferred from computed receiver functions and upper-crustal borehole data respectively (Hakimi and Abdullah, 2014; Korostelev *et al.*, 2015a). The crust was thinned during the last rifting episode during the Oligo-Miocene (Leroy *et al.*, 2012, and references therein).

In the past, magmatism at non-volcanic continental passive margins has commonly been ignored, and the impact of magmatism not expressed at the surface has not been considered when estimating the thermal subsidence history of the margins after breakup. Post-breakup crustal intrusion with limited volcanism after breakup along the highly segmented Gulf of Aden rifted margin is likely maintained by small-scale convection created by the large steps in temperature and lithospheric thickness at the

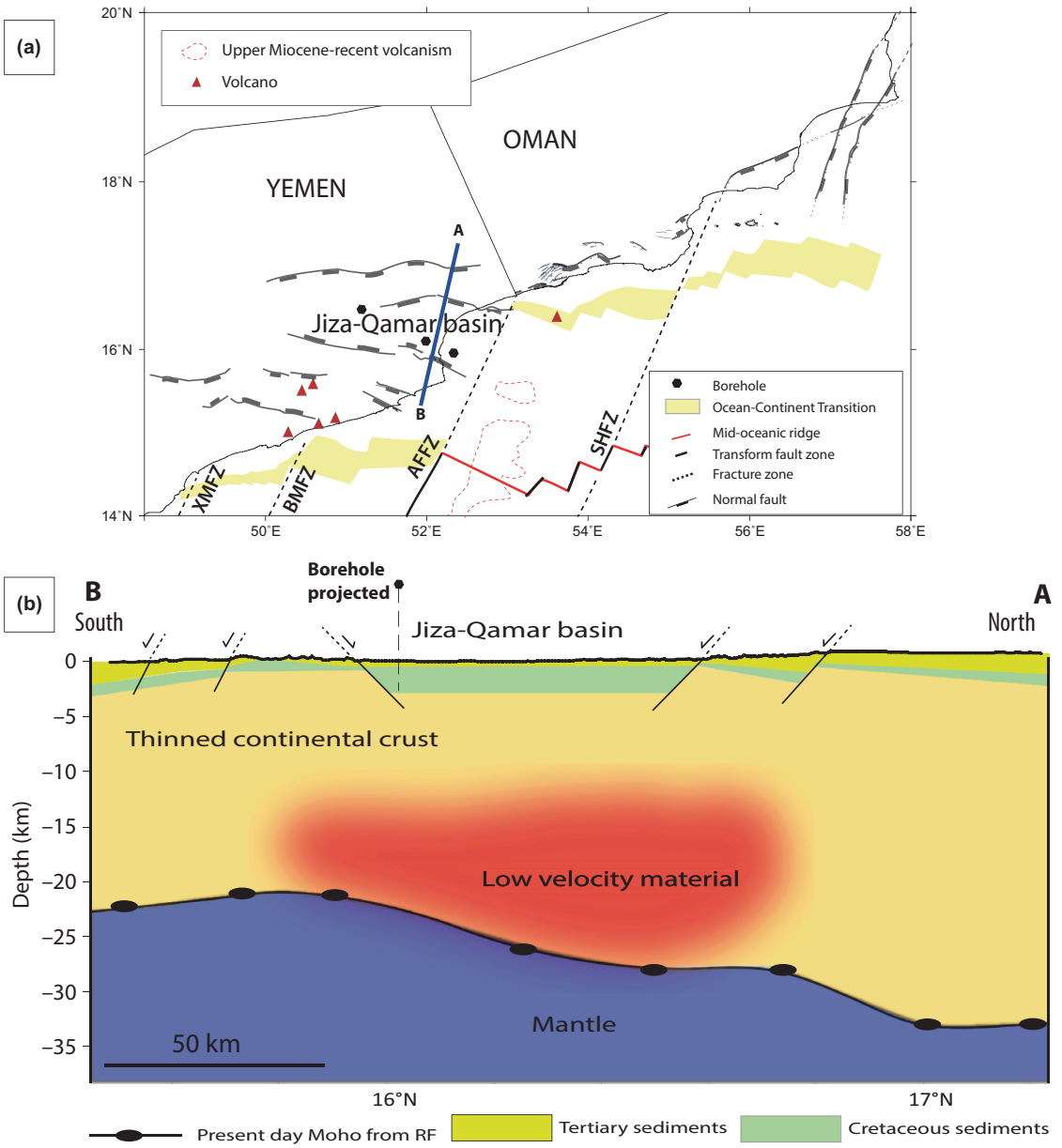

Fig. 4 (a) Location map with simplified tectonic structures, boreholes and cross-section. (b) Schematic cross-section of the Jiza-Qamar basin modified from Brannan *et al.* (1997) and Hakimi and Abdullah (2014). Black dots show Moho depths inferred from receiver functions (Korostelev *et al.*, 2015b). XMFZ, Xiis-Mukalla fracture zone; BMFZ, Bosaso-Masilah fracture zone; AFFZ, Alula-Fartak fracture zone; SHFZ, Socotra-Hadbeen fracture zone.

edge of the Arabian plate (Dumoulin *et al.*, 2008; Lucazeau *et al.*, 2008). Large steps in the topography of the base of the lithosphere are also enhanced in the vicinity of major transform faults, where the juxtaposition of lithosphere of different thermal ages can also trigger small-scale convection (Korostelev *et al.*, 2015a). Channelization of mantle flow from the Afar hotspot along the oceanic ridge and the fracture zones could also be invoked to explain these anomalies (Leroy *et al.*, 2010b; Corbeau *et al.*, 2014). On a local scale, upward magma migration at the rift margin may be aided by pre-existing border faults.

Conclusions

Our study provides new high-resolution phase-velocity maps of the crust and uppermost mantle of the northern margin of the Gulf of Aden using ambient-noise tomography to constrain present-day crustal structure, ~20 Ma after continental breakup.

Low-velocity anomalies are located beneath the Jiza-Qamar (Yemen) and Ashawq-Salalah (Oman) basins and could be caused by ongoing magmatism with no surface expression. This study suggests that magmatism can persist beneath continental passive margins after breakup without being expressed at the surface.

At a lithospheric scale, the ongoing magmatism may be related to small-scale convection at the step in lithospheric thickness beneath the rifted margin, and enhanced by contrasting thicknesses and thermal ages of the lithosphere near fracture zones and transform faults (Korostelev *et al*., 2015a).

Acknowledgements

We acknowledge funding from ANR YOCMAL 07-BLAN-0135, CNRS-INSU-PICS Yemen and Oman, GSMRB Yemen and in the framework of the Actions Marges program (TOTAL, CNRS-INSU, IFREMER, BRGM). We thank Sultan Qaboos University (College of Sciences and Earthquake Monitoring Center), PDO, Oman Geological survey, and the Directorate of Minerals for their help. Seismometers from SEIS-UK are funded by NERC under agreement R8/H10/64. We thank David Hawthorn, Victoria Lane, Christel Tiberi, Francis Lucazeau, François Bache, Mickaël Bonnin, Céline Baurion, Jeffrey Poort and Anna Stork for their efforts during the deployment and servicing of the network. DK is supported by NERC grant NE/L013932/1 and CW by the Netherlands Research Centre for Integrated Solid Earth Science (ISES). We acknowledge constructive comments by P. Poli, an anonymous reviewer and the Associate Editor (A. Gudmundsson) and are grateful to the Editor (C. Doglioni) for the efficient processing of the manuscript.

References

d'Acremont, E., Leroy, S., Beslier, M., Bellahsen, N., Fournier, M., Robin, C., Maia, M. and Gente, P., 2005. Structure and evolution of the eastern Gulf of Aden conjugate margins from seismic reflection data. *Geophys. J. Int*., **160**(3), 869–890.

d'Acremont, E., Leroy, S., Maia, M., Patriat, P., Beslier, M.O., Bellahsen, N., Fournier, M. and Gente, P., 2006. Structure and evolution of the eastern Gulf of Aden: insights from magnetic and gravity data (Encens-Sheba/MD117 cruise). *Geophys. J. Int*., **165**, 786–803.

d'Acremont, E., Leroy, S., Maia, M., Gente, P. and Auti, J.n, 2010. Volcanism, jump and propagation on the Sheba ridge, eastern Gulf of Aden: segmentation evolution and implications for oceanic accretion processes. *Geophys. J. Int*., **180**(2), 535–555.

Ahmed, A., Tiberi, C., Leroy, S., Stuart, G.W., Keir, D., Sholan, J., Khanbari, K., Al-Ganad, I. and Basuyau, C., 2013. Crustal structure of the rifted volcanic margins and uplifted plateau of Western Yemen from receiver function analysis. *Geophys. J. Int*., **193** (3), 1673–1690.

Autin, J., Leroy, S., Beslier, M., d'Acremont, E., Razin, P., Ribodetti, A., Bellahsen, N., Robin, C. and Al Toubi, K., 2010. Continental break-up history of a deep magma-poor margin based on seismic reflection data (northeastern Gulf of Aden margin, offshore Oman). *Geophys. J. Int*., **180** (2), 501–519.

Ayalew, D., Ebinger, C., Bourdon, E., Wolfenden, E., Yirgu, G. and Grassineau, N., 2006. Temporal compositional variation of syn-rift rhyolites along the western margin of the southern Red Sea and northern Main Ethiopian Rift. *Geol. Soc. London Spec. Publ*., **259**(1), 121–130.

Basuyau, C., Tiberi, C., Leroy, S., Stuart, G., Al-Lazki, A., Al-Toubi, K. and Ebinger, C., 2010. Evidence of partial melting beneath a continental margin: case of Dhofar, in the Northeast Gulf of Aden (Sultanate of Oman). *Geophys. J. Int*., **180**(2), 520–534.

Bellahsen, N., Fournier, M., d'Acremont, E., Leroy, S. and Daniel, J.M., 2006. Fault reactivation and rift localization in oblique rifting context: the northeastern Gulf of Aden margin, Sultanate of Oman. *Tectonics*, **25**, 1–14.

Bellahsen, N., Husson, L., Autin, J., Leroy, S. and d'Acremont, E., 2013a. The effect of thermal weakening and buoyancy forces on rift localization: field evidences from the gulf of aden oblique rifting. *Tectonophysics*, **607**, 80–97.

Bellahsen, N., Leroy, S., Autin, J., Razin, P., d'Acremont, E., Sloan, H., Pik, R., Ahmed, A. and Khanbari, K., 2013b. Pre-existing oblique transfer zones and transfer/transform relationships in continental margins: new insights from the southeastern Gulf of Aden, Socotra Island, Yemen. *Tectonophysics*, **607**, 32–50.

Brannan, J., Gerdes, K. and Newth, I., 1997. Tectono-stratigraphic development of the Qamar basin, Eastern Yemen. *Mar. Pet. Geol*., **14**(6), 701–IN12.

Christensen, N. I. and Mooney, W. D., 1995. Seismic velocity structure and composition of the continental crust: a global view. *J. Geophys. Res. Solid Earth*, **100**(B6), 9761–9788.

Corbeau, J., Rolandone, F., Leroy, S., Al-Lazki, A., Keir, D., Stuart, G. and Stork, A., 2014. Uppermost mantle velocity from Pn tomography in the Gulf of Aden. *Geosphere*, **10**, 958–968.

Dumoulin, C., Choblet, G. and Doin, M., 2008. Convective interactions between oceanic lithosphere and asthenosphere: influence of a transform fault. *Earth Planet. Sci. Lett*., **274**(3), 301–309.

Ebinger, C. and Belachew, M., 2010. Geodynamics: active passive margins. *Nat. Geosci*., **3**, 670–671.

Ebinger, C. and Casey, M., 2001. Continental breakup in magmatic provinces: an Ethiopian example. *Geology*, **29**(6), 527–530.

Ferguson, D.J., Maclennan, J., Bastow, I., Pyle, D., Jones, S., Keir, D., Blundy, J., Plank, T. and Yirgu, G., 2013. Melting during late-stage rifting in Afar is hot and deep. *Nature*, **499**(7456), 70–73.

Fry, B., Deschamps, F., Kissling, E., Stehly, L. and Giardini, D., 2010. Layered azimuthal anisotropy of Rayleigh wave phase velocities in the European Alpine lithosphere inferred from ambient noise. *Earth Planet. Sci. Lett*., **297**(1), 95–102.

Gudmundsson, A., 1987. Formation and mechanics of magma reservoirs in Iceland. *Geophys. J. Int*., **91**, 27–41.

Gudmundsson, A., 1995. Stress fields associated with oceanic transform faults. *Earth Planet. Sci. Lett*., **136**, 603–614.

Gudmundsson, A., 2000. Example of Tectonism and Volcanism at Juxtaposed Hot Spot and Mid-OceanRidge Systems. *Annu. Rev. Earth Planet. Sci*., **28**, 107–140.

Gudmundsson, A., 2011. Deflection of dykes into sills at discontinuities and magma-chamber formation. *Tectonophysics*, **500**, 50–64.

Hakimi, M.H. and Abdullah, W.H., 2014. Source rock characteristics and hydrocarbon generation modelling of Upper Cretaceous Mukalla Formation in the Jiza-Qamar Basin, Eastern Yemen. *Mar. Pet. Geol*., **51**, 100–116.

Karato, S. I., 2003. *The dynamic structure of the deep earth: an interdisciplinary approach*. Princeton University Press, Princeton, ISBN: 9780691095110 256 pp.

Korostelev, F., Basuyau, C., Leroy, S., Tiberi, C., Ahmed, A., Stuart, G.W., Keir, D., Rolandone, F., Ganad, I., Khanbari, K., Boschi, L., 2014. Crustal and upper mantle structure beneath south-western margin of the arabian peninsula from teleseismic tomography.

Geochem. Geophys. Geosyst., **15**(7), 2850–2864.
Korostelev, F., Leroy, S., Keir, D., Ahmed, A., Boschi, L., Rolandone, F., Stuart, G., Khanbari, K. and El-Hussain, I., 2015a. Upper mantle structure of the southern Arabian margin: insights from teleseismic tomography. *Geosphere*, **11**, 6.
Korostelev, F.C., Weemstra, S., Leroy, L., Boschi, D., Keir, Y., Ren, I., Molinari, A., Ahmed, G.W., Stuart, F., Rolandone, K., Khanbari, J.O., Hammond, M., Kendall, C., Al Doubre, I., Ganad, B. and Ayele Goitom, A., 2015b. Magmatism on rift flanks: insights from Ambient Noise Phase velocity in Afar region. *Geophys. Res. Lett.*, **42**(7), 2179–2188.
Lebedev, S. and Van Der Hilst, R.D., 2008. Global upper-mantle tomography with the automated multimode inversion of surface and S-wave forms. *Geophys. J. Int.*, **173**(2), 505–518.
Leroy, S., Lucazeau, F., d'Acremont, E., Watremez, L., Autin, J., Rouzo, S., Bellahsen, N., Tiberi, C., Ebinger, C., Beslier, M., Perrot, J., Razin, P., Rolandone, F., Sloan, H., Stuart, G., Al-Lazki, A., Al-Toubi, K., Bache, F., Bonneville, A., Goutorbe, B., Huchon, P., Unternehr, P. & Khanbari, K., 2010a. Contrasted styles of rifting in the eastern Gulf of Aden: a combined wide-angle, multichannel seismic, and heat flow survey. *Geochem. Geophys. Geosyst.*, **11**(7), Q07004.
Leroy, S., d'Acremont, E., Tiberi, C., Basuyau, C., Autin, J., Lucazeau, F. and Sloan, H., 2010b. Recent of-axis volcanism in the eastern Gulf of Aden: implications for plume-ridge interaction. *Earth Planet. Sci. Lett.*, **293** (1), 140–153.
Leroy, S., Razin, P., Autin, J., Bache, F., d'Acremont, E., Watremez, L., Robinet, J., Baurion, C., Denele, Y., Bellahsen, N., Razin, P., Autin, J., Bache, F., d'Acremont, E., Watremez, L., Robinet, J., Baurion, C., Denèle, Y., Bellahsen, N., Lucazeau, F., Rolandone, F., Rouzo, S., Serra Kiel, J., Robin, C., 2012. From rifting to oceanic spreading in the Gulf of Aden: a synthesis. *Arab. J. Geosci.*, **5**, 859–901.
Lucazeau, F., Leroy, S., Bonneville, A., Goutorbe, B., Rolandone, F., d'Acremont, E., Watremez, L., Düsünur, D., Tuchais, P., Huchon, P., Bellahsen, N. and Al-Toubi, K., 2008. Persistent thermal activity at the Eastern Gulf of Aden after continental break-up. *Nature Geosci.*, **1**, 854–858.
Lucazeau, F., Leroy, S., Autin, J., Bonneville, A., Goutorbe, B., Watremez, L., d'Acremont, E., Dusunur, D., Rolandone, F., Huchon, P., Bellahsen, N. and Tuchais, P., 2009. Post-rift volcanism and high heat-flow at the ocean-continent transition of the eastern Gulf of Aden. *Terra nova*, **21** (4), 285–292.
Lucazeau, F., Leroy, S., Rolandone, F., d'Acremont, E., Watremez, L., Bonneville, A., Goutorbe, B. and Dusunur, D., 2010. Heat-flow and hydrothermal circulation at the ocean continent transition of the eastern Gulf of Aden. *Earth Planet. Sci. Lett.*, **295** (3), 554–570.
Manetti, P., Capaldi, G., Chiesa, S., Civetta, L., Conticelli, S., Gasparon, M., Volpe, L. and Orsi, G., 1991. Magmatism of the eastern Red Sea margin in the northern part of Yemen from Oligocene to present. *Tectonophysics*, **198**(2), 181–202.
McKenzie, D., 1978. Some remarks on the development of sedimentary basins. *Earth Planet. Sci. Lett.*, **40**(1), 25–32.
Pallister, J., McCausland, W., Jonsson, S., Lu, Z., Zahran, H., El Hadidy, S., Aburuk, A. buruk bah, Stewart, I., Lundgren, P., White, R. and Moufti, M., 2010. Broad accommodation of rift-related extension recorded by dyke intrusion in Saudi Arabia. *Nature Geosci.*, **3**, 705–712. doi:10.1038/NGEO966.
Pasyanos, M.E. and Nyblade, A.A., 2007. A top to bottom lithospheric study of Africa and Arabia. *Tectonophysics*, **444**, 27–44.
Robinet, J., Razin, P., Serra-Kiel, J., Gallardo-Garcia, A., Leroy, S., Roger, J. and Grelaud, C., 2013. The Paleogene pre-rift to syn-rift succession in the Dhofar margin (northeastern Gulf of Aden): stratigraphy and depositional environments. *Tectonophysics*, **607**, 1–16.
Rolandone, F., Lucazeau, F., Leroy, S., Mareschal, J.-C., Jorand, R., Goutorbe, B. and Bouquerel, H., 2013. New heat flow measurements in Oman and the thermal state of the Arabian Shield and Platform. *Tectonophysics*, **589**, 77–89.
Rooney, T., Herzberg, C. and Bastow, I., 2012. Elevated mantle temperature beneath East Africa. *Geology*, **40** (G32382R1), 27–40.
Rooney, T., Bastow, I., Keir, D., Mazzarini, F., Movsesian, E., Grosfils, E., Zimbelman, J., Ramsey, M., Ayalew, D. and Yirgu, G., 2014. The protracted development of focused magmatic intrusion during continental rifting. *Tectonics*, **33**, 1–23.
Ryan, W.B.F., Carbotte, S.M., Coplan, J.O., O'Hara, S., Melkonian, A., Arko, R., Weissel, R.A., Ferrini, V., Goodwillie, A., Nitsche, F., Bonczkowski, J. and Zemsky, R., 2009. Global Multi-Resolution Topography synthesis. *Geochem. Geophys. Geosyst.*, **10**, Q03014.
Stab, M., Bellahsen, N., Pik, R., Quidelleur, X., Ayalew, D. and Leroy, S., 2015. Mode of rifting in magma-rich settings: tectono-magmatic evolution of Central Afar. *Tectonics*, DOI: 10.1002/2015TC003893
Tard, F., Masse, P., Walgenwitz, F. and Gruneisen, P., 1991. The volcanic passive margin in the vicinity of Aden, Yemen. *Bull. Centres Rech. Explor.-Prod. Elf-Aquitaine*, **15**, 1–9.
Tiberi, C., Leroy, S., d'Acremont, E., Bellahsen, N., Ebinger, C., Al-Lazki, A. and Pointu, A., 2007. Crustal geometry of the northeastern Gulf of Aden passive margin: localization of the deformation inferred from receiver function analysis. *Geophys. J. Int.*, **168** (3), 1247–1260.
Watremez, L., Leroy, S., Rouzo, S., d'Acremont, E., Unternehr, P., Ebinger, C., Lucazeau, F. and Al-Lazki, A., 2011. The crustal structure of the north-eastern Gulf of Aden continental margin: insights from wide-angle seismic data. *Geophys. J. Int.*, **184** (2), 575–594.
Watremez, L., Burov, E., d'Acremont, E., Leroy, S., Huet, B., Pourhiet, L. and Bellahsen, N., 2013. Buoyancy and localizing properties of continental mantle lithosphere: insights from thermomechanical models of the eastern Gulf of Aden. *Geochem. Geophys. Geosyst.*, **14**(8), 2800–2817.
Wolfenden, E., Ebinger, C., Yirgu, G., Renne, P. and Kelley, S., 2005. Evolution of a volcanic rifted margin: Southern Red Sea, Ethiopia. *Geol. Soc. Am. Bull.*, **117**(7–8), 846–864.

Received 8 April 2015; revised version accepted 16 September 2015

Supporting Information

Additional Supporting Information may be found in the online version of this article:

Data S1. Data, method and resolution tests

